NEMoSys: A Platform for Adaptive Mesh Refinement and Solution Verification

Sachin R. Natesh,[1] Masoud Safdari,[1]

[1]*Illinois Rocstar LLC, 108 Hessel Blvd., Champaign, Illinois, 61820-6574, USA,* tech@illinoisrocstar.com

INTRODUCTION

During the past twenty years, breakthroughs in numerical analysis and the advent of high performance computing have driven forward the state-of-the-art in nuclear reactor modeling and simulation (M&S). High fidelity M&S is increasingly critical to cost-effective design and advanced safety modeling of nuclear reactors, and several, advanced M&S tools, such as the *SHARP* (Simulation for High-efficiency Advanced Recator Protoyping) [1] framework and *Nek5000* [2] have formed to address this criticality. However, deterministic simulations of complete nuclear reactor cores remains a challenge due to the multitude of fuel assemblies within a core [3] and the concurrent need for resolving small, yet important geometric features, such as mixing vanes and wire wraps [4]. Several types of high-fidelity numerical schemes require "meshes" or, equivalently, "grids". A mesh is a discretization of the spatial domain in which the considered physical process occurs into simple geometries that are more amenable to numerical analysis. The quality of these numerical schemes relies on the quality and density of the discretization. A dense enough mesh can capture important geometric features and accurately reproduce characteristics of the governing dynamical systems; however, achieving high resolution may be prohibitive in its computational expense. The processes of generating a mesh that is best suited to efficiently and accurately approximate the solution to a given problem constitutes a major bottleneck in mesh-based simulation workflows, often consuming upwards of 80% of total analysis time [5]. Moreover, appropriate verification and validation (V&V) of simulation software, models and solutions is of paramount importance to M&S society, especially to nuclear regulators and industry. While all stages of V&V are laborious and resource consuming, the grid manipulations required during *solution verification* are mostly carried out manually, and the analyses conducted are often reliant on experience as well as heuristics established by trial-and-error.

Adaptive mesh refinement (AMR) can address, in an "intelligent" fashion, the polarity between accuracy and efficiency in mesh-based numerical simulations. Since the 1970s, these techniques have been applied to different classes of partial differential equations (PDEs) and proven powerful in decreasing the resolution of spatial discretization, while achieving a comparable, if not superior, level of accuracy in the computed solution [6]. AMR methods enhance the quality and efficiency of an initial, mesh-based, numerical approximation through modulation of the number of degrees of freedom in regions of the domain identified by error criteria and have been identified as a primary development objective for numerical methods in nuclear M&S [7]. Unfortunately, the realization of an AMR scheme is plagued by the bottleneck of quality mesh generation.

There exist several open-source software tools for mesh generation, such as *Gmsh* [8], *Netgen*, and *TetGen*. While capable and robust, these packages are characterized by steep learning curves and do not natively support the automation desired in an AMR scheme. Moreover, they lack the tools needed for accurately and conservatively transferring solution and boundary condition data between AMR iterations. Despite the benefits of AMR in mesh-based M&S, there exist few commercial, off-the-shelf, or open-source software solutions for its general purpose application. This is, in part, due to the diversity of tools required as well as the heterogeneity of AMR techniques, which are distinguished by the criteria used to identify refinement locations, the underlying discretization method, and the physics of the problem. Some end-to-end, open-source simulation packages, such as the finite element codes *MFEM* [9] and *MOOSE* [10], natively support the incorporation of AMR in their solvers; however, the routines are not easily incorporable with external solver libraries using different discretization methods. As far as solution verification is concerned, no general-purpose frameworks exist, for assessing convergence of and establishing confidence in the computed numerical solution. While high fidelity benchmarks can be used for this purpose, as in [11], they are specific to the equations of the model and usually rely on the provision of an analytic solution.

In the present article, we report on the development of the **N**uclear **E**nergy **Mo**deling **Sys**tem (*NEMoSys*) - a modular, extensible platform for robust, automated AMR and solution verification. Built on top of several open-source libraries, including *Gmsh*, the Data Transfer Kit (*DTK*) [12], and the Mesh Adaptation Library (*MAdLib*) [13], *NEMoSys* will ultimately serve AMR and solution verification methodologies to nuclear M&S software, including *Nek5000*, *PROTEUS* [14], and *MFEM*. It facilitates prudent solution verification for arbitrary polyhedral meshes and anisotropic AMR schemes for triangular and tetrahedral element meshes. The general-purpose utility of *NEMoSys* stems from our identification and abstraction of the commonalities between AMR techniques and implementation of a general, Richardson extrapolation-based solution verification module. In the remainder of the paper, we briefly discuss the theoretical basis of the AMR and solution verification methods implemented in *NEMoSys* and showcase the package's capabilities with demonstrative case studies.

THEORY AND IMPLEMENTATION

AMR, Error Criteria and Size Fields

Generally, there are three fundamental steps which are performed during an AMR scheme: the evaluation of refinement criteria, refinement of the mesh and the transfer of physical quantities from the original to the refined mesh. In *NEMoSys*, the first step results in a *Size Field*, $\delta(\mathbf{x})$, which defines target element sizes at each point of the mesh. Size fields are defined by *a-posteriori* error estimators, error indicators and possibly

naive criteria, such as the value or gradient of a solution field. They are used to guide the mesh adaptation through a series of local mesh modifications; namely, edge splitting, vertex collapse, edge swaps and face swaps. For value or gradient-based criteria, we normalize the chosen solution field or its gradient, component-wise by its mean value, take the reciprocals of each normalized value and apply the following feature scaling to realize the size field:

$$\delta(\mathbf{x}) = h_{\min} + \frac{(h_{\max} - h_{\min})(v(\mathbf{x}) - v_{\min})}{v_{\max} - v_{\min}}, \tag{1}$$

where $h_{\min}$ and $h_{\max}$ are the min and max diameters of the circumspheres of elements in the mesh, respectively, and $v(\mathbf{x})$ is the reciprocated, normalized value (or gradient magnitude) at grid point x. A user-defined, size field multiplier can further control the scaling.

Concerning error indicators and estimators, we have implemented the Zienkiewicz-Zhu (Z2) error indicator, which, when optimal sampling points are available, serves as an estimator as well [15]. We recover potentially more accurate nodal values for a given solution field and approximate the error in element i by

$$\|\boldsymbol{e}_{\sigma,i}\|_{L_2} = \left(\int_{\Omega_i} (\boldsymbol{\sigma}^\star - \hat{\boldsymbol{\sigma}})^T (\boldsymbol{\sigma}^\star - \hat{\boldsymbol{\sigma}}) d\Omega \right)^{\frac{1}{2}}, \tag{2}$$

where $\boldsymbol{\sigma}^\star$ and $\hat{\boldsymbol{\sigma}}$ are the recovered and original nodal values, respectively. Then, we define the absolute, root mean square error (RMSE) in element i with

$$\Delta\boldsymbol{\sigma}_i = \left(\frac{\|\boldsymbol{e}_{\sigma,i}\|_{L_2}^2}{|\Omega_i|} \right)^{\frac{1}{2}}, \tag{3}$$

where $|\Omega_i|$ is the volume of element i. Using Eq. 3, we can define a sensible target element size given the RMSE and the order of the problem p:

$$\begin{aligned} h_i^\star &= \frac{h_i}{\xi_i^{\frac{1}{p}}} = \sum_{j=1}^{n_i} \delta(\mathbf{x_j}) w_j, \\ \xi_i &= \frac{\Delta\boldsymbol{\sigma}_i}{\Delta\overline{\boldsymbol{\sigma}}}, \end{aligned} \tag{4}$$

where $\Delta\overline{\boldsymbol{\sigma}}$ is the maximal permissible error. This can be set *a priori* or determined based on moments of the element distribution of $\Delta\boldsymbol{\sigma}_i$. The right-hand equality at the top of Eq. 4 provides the relation between the element size and the size field, where n_i is the number of nodes in element i, and w_j are the shape function weights evaluated at the center of the element.

With the size fields defined, an h-refinement process is started wherein the resulting meshes' element size distribution is steered towards optimal consistency with the size field, constrained by permitted changes to the topology of the mesh. Then, we transfer the solution from the original mesh to the adaptively refined mesh via standard, consistent interpolation.

Autonomous Solution Verification

The discretization error of a numerical solution to a PDE is the difference between the approximate solution, $\hat{f}_k$, obtained from grid/mesh k and exact value given by

$$\delta_d = \hat{f}_k - f_{exact} = g_p h^p + HOT, \tag{5}$$

where g_p is the coefficient of the leading order term and p is the observed order of accuracy. Generalized Richardson extrapolation theory can be used to perform automated solution verification based on a systematic grid refinement approach. The method relies on three major assumptions: i) the solution is smooth, ii) higher-order terms are small, and iii) uniformly refined meshes are used. Given three meshes with refinement factors $r_{21} = h_2/h_1 > 1$, $r_{32} = h_3/h_2 > 1$, and $r_{21} \neq r_{32}$, the observed order or accuracy can be obtained by solving the transcendental equation given by

$$\frac{f_3 - f_2}{r_{32}^p - 1} = r_{21}^p \left[\frac{f_2 - f_1}{r_{21}^p - 1} \right], \tag{6}$$

using an iterative procedure. When the solution is in the asymptotic convergence range, the value of p should be close to the formal order of accuracy.

Another criterion for solution verification is Roache's grid convergence index (GCI) [16], defined for solutions f_1 and f_2 as

$$GCI_{21} = \frac{F_s}{r_{21}^p - 1} \left| \frac{f_2 - f_1}{f_1} \right|, \tag{7}$$

where F_s is a safety factor. The GCI represents an error band within which the converged numerical solution exists with a 95% confidence level. That is, we can say with 95% confidence that the converged numerical solution lies within the interval $[f_1(1 - \mathrm{GCI}_{21}), f_1(1 + \mathrm{GCI}_{21})]$. It is based on generalized Richardson extrapolation theory and therefore works best when its assumptions are valid.

One advantage of the GCI is that it only requires two numerical solutions (f_1 and f_2). The GCI also requires knowledge of the order of accuracy (p), which can be a disadvantage. When only a nominal order of accuracy is known, the safety factor should be $F_s = 3.0$. In the case of three available solutions, the safety factor should be $F_s = 1.25$. In the considered case, the GCI can be used to assert that the solutions are in the asymptotic range of convergence. Because of GCI's basis in generalized Richardson extrapolation theory, the error in the GCI relative to the exact discretization error, normalized by the exact solution, tends to 0 as $h \to 0$. Thus, the following relation between the two GCIs computed over the three meshes must hold, for some small ϵ, if the solutions are in the asymptotic range of convergence:

$$\left| \frac{\mathrm{GCI}_{32}}{\mathrm{GCI}_{21} r_{21}^p} - 1 \right| < \epsilon. \tag{8}$$

Once the relation in Eq. 8 is established, it can be used to approximate the grid resolution r^* required for some acceptable GCI^* by way of If the goal of a solution verification study is to 1) quantify the error in the solution due to spatial discretization and 2) determine the grid resolution necessary to achieve some desired or acceptable discretization error, it is imperative to have proper knowledge of the order of accuracy and existence of solutions within the asymptotic convergence range.

DEMONSTRATIVE CASE STUDIES

AMR for Wave Propagation in a Solid

In this case study, we investigate the application of AMR to wave propagation in a beam. A cantilever beam is clamped at one end and subjected to displacement and velocity functions $u(t) = u_1(1)$ and $v(t) = v_1(1)$ at the other end. We subject the beam to linear displacement and step velocity profiles and solve a dynamic linear elasticity problem using a linear tetrahedral element discretization and *MFEM* for computation. We use a 3-stage *Runge-Kutta* (RK3) scheme for stepping the problem in time, with time step $\delta t = 10\,\mu s$. A wave formed in the right end propagates through the beam, hitting the fixed side, then reflects back. The objective of this study is to investigate the degree to which AMR can assist in reducing the dimensionality of the problem discretization, and thereby, reduce computational expense. The initial mesh used for the problem is too coarse to resolve the important frequencies of the wave in which we are interested. We can use globally fine meshes to resolve those frequencies; however, that would increase the computational cost of the problem. Instead, we employ AMR to reduce the cost. We note that in this problem, the most important zone is at the forefront of the wave. To capture only the wave front, we use the velocity component v_1 as the criterion for value-based AMR. Figure 1 illustrates application of this AMR technique. The refinement is concentrated only around the zone of interest. We have substantially reduced computational expense and obtain accurate results without manually changing the mesh as the simulation progresses in time.

We note that one of the major quantities that we are interested in is the strain. Since the strain is not directly solved for, but calculated during post-processing from the gradient of the displacement field, we use the magnitude of the gradient of u_1 as the refinement criteria for AMR. Figure 2 illustrates the adaptively refined mesh and solution field as we progress in time.

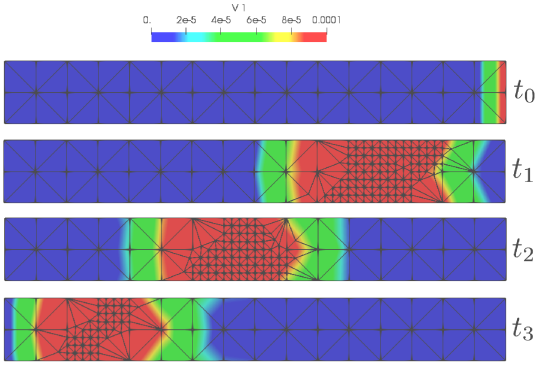

Fig. 1. AMR using velocity component v_1 to create the size field. A face of the beam is shown.

Solution Verification of a Problem in Linear Elasticity

In this study, we consider a simple linear elasticity problem that describes a bi-material, cantilever beam with a constant, uniform pull-down force applied to the boundary elements of one material and 0 load applied to the other. We employ a finite element discretization with linear triangular and tetrahedral elements to solve for the deformation of the beam. We conduct two spatial convergence studies, herein referred to as 'asymptotic' and 'non-asymptotic', each involving three solutions (nodal displacements) on successively refined meshes. The solutions are computed with *MFEM*. Table I provides the number of points and cells in each mesh within each study.

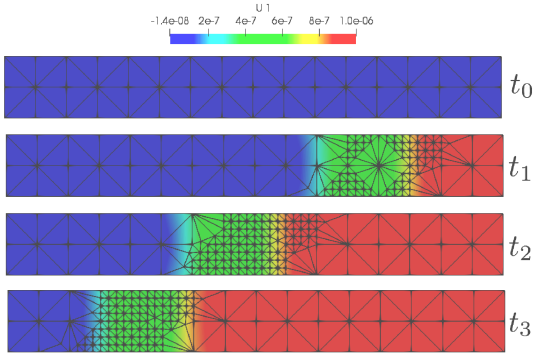

Fig. 2. AMR using the gradient of displacement component u_1 to create the size field. A face of the beam is shown.

TABLE I. Grids Used in Convergence study

	Non-Asymptotic		**Asymptotic**	
	Cells	Points	Cells	Points
f_0	12,861,440	2,167,425	12,861,440	2,167,425
f_1	4,160	825	1,642,496	279,873
f_2	656	153	214,016	37,281
f_3	116	36	28,928	5,265

We adopt a solution numbering convention wherein smaller subscripts indicate solutions on finer grids. It is important to note that f_0 is computed on a very fine mesh and is the same across both studies. It will be used as a proxy to the exact solution to measure discretization errors when the conditions for Richardson extrapolation are not met. We compute the GCI ratios, with $F_s = 1.5$ and check there proximity to unity, as indicated by Eq. 8. We also calculate the observed order of accuracy obtained from each study. For the non-asymptotic study, the GCI ratio and observed order of accuracy are 1.387 and 1.085, respectively. For the asymptotic study, the ratio and observed order are 1.00 and 2.00, respectively.

Not only is the GCI ratio for the non-asymptotic study not particularly close to unity, but the observed order of accuracy is far from the expected, formal order $p = 2$. To highlight the importance of prior knowledge concerning the convergence behavior of solutions used in a verification study, consider Figure 3. The global L^2-norms of the discretization error of the displacement in the z direction are plotted against the characteristic mesh size h on a log-log scale. On this scale, the slopes represent the observed order of accuracy. If the solutions are asymptotically converged, linear interpolation will allow prediction of the mesh size required for a prescribed discretization error. In Figure 3, these predictions are represented by the star ($\star$) markers. The discretization error is chosen to be $\|f_0 - f_1\|_{L^2}$. The expected h is h_1, and the expected error-h

pairs are represented by the square markers. The asymptotic

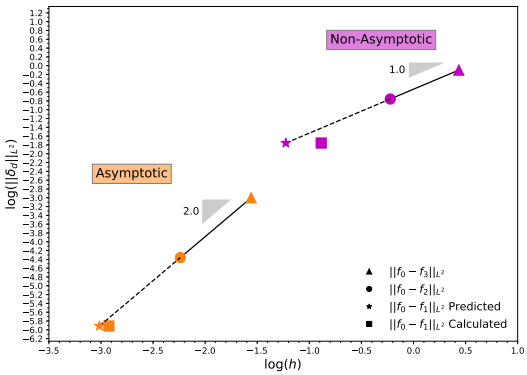

Fig. 3. Global L^2-norms of the discretization error in z-displacement, computed using f_0.

solutions predict an h value that differs from the actual h value by 8.7%, while the non-asymptotic solutions predict an h that differs from the actual by 28.8%. The larger prediction error for the non-asymptotic study stems from the mismatch between the observed order of accuracy (here ~ 1.1) and the expected formal order of 2. Furthermore, the erroneously smaller h value for the prescribed discretization error results in unnecessary computational expense from generation of a finer grid than needed to achieve the desired level of accuracy.

So, with the solution verification module in *NEMoSys*, users can provide three grids with solutions, check for asymptotic convergence and predict the refinement level required to achieve near a desired level of accuracy.

CONCLUSIONS

The work presented in this paper describes the development of *NEMoSys*, a framework for automated adaptive mesh refinement and solution verification. In the wake of reactor license expiration and the need for development of new reactors with advanced safety features, *NEMoSys* contributes to the increasingly relevant goal of improving the accuracy and efficiency of high-fidelity nuclear reactor core and plant M&S. We demonstrated the use of the AMR module for wave propagation in a solid using value-based methods for determining refinement locations. The AMR technique was shown, qualitatively, to balance the resolution of the discretization and accuracy of results obtained. We also demonstrated the capabilities of the solution verification module for a simple, static beam deformation problem, and, in particular, how the module can be used to generate grids refined to a level that will achieve a desired accuracy with minimal user intervention. Future work includes extending the AMR module to support arbitrary, polyhedral meshes, providing support for parallel computation and the development of error estimation methodologies relevant to nuclear M&S.

ACKNOWLEDGMENTS

This work has been funded by a DOE Phase I SBIR grant, No. DE-SC0018077 and by Illinois Rocstar LLC.

REFERENCES

1. P. FISCHER, D. KAUSHIK, D. NOWAK, W. SIEGEL, W. YANG, and G. PIEPER, "Advanced Simulation for Fast Reactor Analysis," *SciDAC Review* (2008).
2. P. FISCHER, J. LOTTES, and S. KERKEMEIER, "nek5000 Web page," (2008), http://nek5000.mcs.anl.gov.
3. F. ROELOFS, V. GOPALA, L. CHANDRA, M. VIELLIEBER, and A. CLASS, "Simulating fuel assemblies with low resolution CFD approaches," *Nuclear Engineering and Design*, **250**, 548–559 (Sep. 2012).
4. P. F. FISCHER, J. W. LOTTES, A. R. SIEGEL, and G. PALMIOTTI, "Large Eddy Simulation of Wire-Wrapped Fuel Pins: Hydrodynamics of a Single Pin," (2007).
5. Y. BAZILEVS, V. CALO, J. COTTRELL, J. EVANS, T. HUGHES, S. LIPTON, M. SCOTT, and T. SEDERBERG, "Isogeometric analysis using T-splines," *Computational Geometry and Analysis*, **199**, *5–8*, 229–263 (Jan. 2010).
6. M. J. BERGER and J. OLIGER, "Adaptive mesh refinement for hyperbolic partial differential equations," *Journal of Computational Physics*, **53**, *3*, 484–512 (Mar. 1984).
7. P. FINCK, D. KEYES, and R. STEVENS, "Workshop on Simulation and Modeling for Advanced Nuclear Energy Systems," (Aug. 2006).
8. C. GEUZAINE and J. REMACLE, "Gmsh: A 3D finite element mesh generator with built-in pre- and post-processing facilities," *International Journal for Numerical Methods in Engineering*, **79**, *11*, 1309–1331 (Aug. 2009).
9. "MFEM: Modular Finite Element Methods Library," `mfem.org`.
10. D. GASTON, C. NEWMAN, G. HANSEN, and D. LEBRUN-GRANDIE, "MOOSE: A Parallel Computational Framework for Coupled Systems of Nonlinear Equations," *Nucl. Eng. Des.*, **239**, 1768 – 1778 (2009).
11. B. GANAPOL, M. DEHART, F. GLEICHER, J. ORTENSI, S. SCHUNERT, and R. MARTINEAU, "HTR-10 Multiphysics Point Kinetics Benchmark," *M&C 2017* (2017).
12. "The Data Transfer Kit: A Geometric Rendezvous-Based Tool for Multiphysics Data Transfer," (Jul. 2013).
13. G. COMPÃĹRE, J.-F. REMACLE, J. JANSSON, and J. HOFFMAN, "A mesh adaptation framework for dealing with large deforming meshes," **82**, 843 – 867 (May 2010).
14. M. SMITH, C. RABITI, G. PALMIOTTI, D. KAUSHIK, A. SIEGEL, B. SMITH, T. TAUTGES, and W. YANG, "UNIC: Development of a New Reactor Physics Analysis Tool," *Trans. Am. Nucl. Soc.*, **97**, 565 – 566 (2007).
15. O. ZIENKIEWICZ and J. ZHU, "The Superconvergent Patch Recovery And *A Posteriori* Error Estimates. Part 1: The Recovery Technique," *International Journal for Numerical Methods in Engineering*, **33**, 1331–1364 (1982).
16. P. J. ROACHE, "Perspective: a method for uniform reporting of grid refinement studies," *Transactions-American Society of Mechanical Engineers Journal of Fluids Engineering*, **116**, 405–405 (1994).